INFLUENCE OF SPATIAL DISTRIBUTION OF ROUGHNESS ELEMENTS ON TURBULENT FLOW PAST A BIOFOULED SURFACE

Sotirios Sarakinos
James Watt School of Engineering
University of Glasgow
Glasgow G12 8QQ, United Kingdom
sotirios.sarakinos@glasgow.ac.uk

Angela Busse
James Watt School of Engineering
University of Glasgow
Glasgow G12 8QQ, United Kingdom
angela.busse@glasgow.ac.uk

ABSTRACT

In most fundamental studies on the effect of roughness elements on wall-bounded turbulence regular arrangements of roughness elements are investigated. In this study, direct numerical simulations are used to study the flow past irregular rough surfaces composed of barnacle-type roughness elements. The aim is to assess the influence of clustering, i.e. non-uniform distribution, of the roughness-elements on near-wall turbulence.

Three surfaces covered with random arrangements of a population of barnacles with the same planform and frontal solidities, but differing degrees of clustering, have been investigated using direct numerical simulations of turbulent channel flow at $Re_\tau = 395$. For comparison, a simulation over a classical staggered arrangement of barnacle elements of uniform size with matching planform and frontal solidity has been conducted. Surfaces with a high degree of clustering yield a lower roughness function ΔU^+ compared to surfaces that are more homogeneously covered by roughness elements. The staggered arrangement yields a value for the roughness function that is comparable to a homogeneous random distribution of barnacles with a low degree of clustering.

Clustering also affects the levels of the Reynolds and dispersive stresses in the near-wall region, with strongly clustered arrangements leading to elevated spanwise and wall-normal Reynolds stresses and the highest levels of dispersive normal stresses above the rough surface. Visualisations of the time-averaged streamwise velocity field show a clear interaction between barnacles within a closely packed cluster, leading to strong shielding effects for barnacles with upstream neighbours, and a merging of wakes. Overall, closely clustered barnacles form a 'super-obstacle' and thus interact differently with the near-wall flow compared to surfaces where roughness elements are clearly segregated from each other and interact with the flow on an individual basis. On the other hand, a classical, regular staggered arrangement of roughness elements serves as good proxy of non-clustered random arrangements of roughness elements when considering mean-flow statistics.

INTRODUCTION

Marine biofouling has affected seafaring since ancient times by decreasing the maximum speed and range of ships (Schultz *et al.*, 2011). When marine organisms start to accumulate on a ship hull, the skin friction drag of the hull rises rapidly, increasing the fuel burn and associated emissions such as carbon dioxide and noxious or sulphurous gases. Calcareous macrofouling, caused by organisms protected by a calcareous outer shell, is considered the form of marine biofouling with the most severe consequences for the shipping industry.

Barnacles are one of the most common forms of calcareous macrofouling. Barnacles start their life-cycle as swimming larvae. When maturing, the larvae search for a surface to settle on permanently. Once settled on a surface, they build a calcareous protective shell around their body that is securely fixed to the supporting surface. Barnacles tend to settle next to other barnacles to gain good feeding grounds and conditions for reproduction by forming colonies (Knight-Jones & Crisp, 1953).

Previous research on barnacle-type macrofouling has mainly been based on experiments on plates that were exposed for longer periods of time to biofouling conditions (see e.g. Schultz (2004)). Furthermore, flow over surfaces covered by ordered arrays of barnacle-like shapes has been investigated both numerically (Sadique *et al.*, 2015) and experimentally (Barros *et al.*, 2016). However, a regular arrangement of barnacles does not closely match realistic barnacle fouled surfaces as barnacles tend to form clusters when they colonise a surface. In the current work, a range of irregular barnacle-type rough surfaces are investigated focusing on the effect of increasing clustering of roughness elements on the roughness function and near-wall turbulence levels.

METHODOLOGY

Three different rough surfaces with irregular barnacle roughness have been investigated using direct numerical simulations of turbulent channel flow. An additional rough

surface where barnacles were placed in a classical regular staggered arrangement was added for comparison.

Surface generation

The shape of a barnacle can be approximated by a conical frustum (Sadique *et al.*, 2015). Using an algorithm that mimics the settlement of barnacles (Sarakinos & Busse, 2019), three different irregular, barnacle-type rough surfaces have been generated with varying degrees of proximity between the barnacles. All three surfaces, shown in figure 1(a)-(c), were generated using the same set of 44 barnacles, which have a distribution of heights and diameters that mimics a realistic barnacle population. The minimum barnacle height h^b_{min} and maximum barnacle height h^b_{max} are given in table 1. The average barnacle height h^b_{ave} is $h^b_{ave} = 0.092\delta$, where δ is the mean channel half-height. Case 1 has the highest degree of clustering with several distinct barnacle clusters. In case 2, the clusters are more loosely connected, but still discernible. Case 3 has the lowest degree of clustering with a uniform, homogeneous random distribution of barnacles over the surface where no clusters can be distinguished. As the same barnacle population has been used for all three surfaces, they have identical rms roughness height Sq, coverage percentage/planform solidity λ_p, and frontal solidity λ_f (see table 1). The skewness of the surfaces is high with $Ssk = 4.07$. This is typical of surfaces with sparse coverage by roughness elements.

Table 1. Parameters describing the barnacle shape and the topography of the rough surfaces

case	Sq	h^b_{min}/δ	h^b_{max}/δ	λ_p	λ_f
1 to 3	0.018	0.068	0.127	10%	0.034
staggered	0.016	0.088	0.088	10%	0.034

For comparison, a surface with regular barnacle-type roughness was generated by placing 50 barnacles of the same shape and size in a classical staggered arrangement reminiscent of the regular rough surfaces studied by Schlichting (1936). The dimensions of the barnacle were adjusted to closely match key topographical parameters of the irregular surfaces, while maintaining a realistic barnacle shape. The regular staggered surface has the same planform and frontal solidity, and the height of the barnacle element is close to the average height of the barnacle population of the irregular cases. The skewness of the staggered surface is $Ssk = 3.92$, i.e. the difference in skewness between the regular and irregular cases is less than 5%.

Numerical simulations

Direct numerical simulations of turbulent channel flow at $Re_\tau = 395$ with a constant mean streamwise pressure gradient were conducted for the rough surfaces described above. The surface roughness was applied to both the lower and the upper wall of the channel and resolved using an embedded boundary method (Busse *et al.*, 2015).

To maintain a constant mean channel half height δ for all cases, a small vertical offset z_0 was applied in the

rough-wall cases to the smooth surface on which the roughness elements were placed. The roughness mean plane, i.e. $\langle h(x,y)\rangle$, where $h(x,y)$ is the local elevation of the rough surface as a function of the streamwise (x-) and the spanwise (y-) coordinate, thus corresponds to $z = 0$, where z is the wall-normal coordinate. The domain size is $2\pi\delta$ in the streamwise and $\pi\delta$ in the spanwise direction. A grid size of $864 \times 432 \times 512$ was used for all rough cases. Uniform grid spacing was employed in the streamwise and spanwise direction. In the wall-normal direction a constant grid spacing of Δz^+_{min} was used for $z \leq \max(h(x,y))$, and the grid stretched gradually above reaching its maximum spacing Δz^+_{max} at the channel centre (see table 2). The smooth-wall simulation data are taken from a previous study conducted at the same Reynolds number using the same simulation code (Jelly & Busse, 2018).

Table 2. Numerical simulation parameters

case	Δx^+	Δy^+	Δz^+_{min}	Δz^+_{max}	z_0/δ
1 to 3	2.87	2.87	0.67	3.11	-0.0050
staggered	2.87	2.87	0.5	2.73	-0.0054

RESULTS

All surfaces yield a roughness function ΔU^+ that falls into the upper transitionally rough regime (see Table 3). Case 1, with the strongest clustering of barnacles, yields the lowest ΔU^+ that is $\approx 20\%$ lower than for case 3, where the barnacles follow a uniform random distribution. Increasing clustering of barnacle roughness elements there-

Table 3. Roughness function ΔU^+

case	case 1	case 2	case 3	regular
ΔU^+	4.93	5.64	6.17	6.15

fore decreases the fluid dynamic roughness effect of a surface. This may be a consequence of improved shielding effects within a more closely packed barnacle cluster. The roughness function ΔU^+ of the regular, staggered surface closely matches the roughness function of case 3. A classical staggered arrangement of roughness elements can thus serve as a reasonable proxy for an irregular rough surface where roughness elements are distributed in a uniform random manner. However, a regular staggered arrangement will overpredict the roughness effect of a strongly clustered surface.

The profiles of the mean flow and turbulence statistics shown in the following have been computed using the 'intrinsic' average, i.e. below the highest roughness height $z \leq \max(h(x,y))$ the spatial average is taken only over the fluid occupied area at a given wall-normal location z and no 'superficial' average is employed. The mean streamwise velocity profiles (see figure 2) show that the logarithmic layer
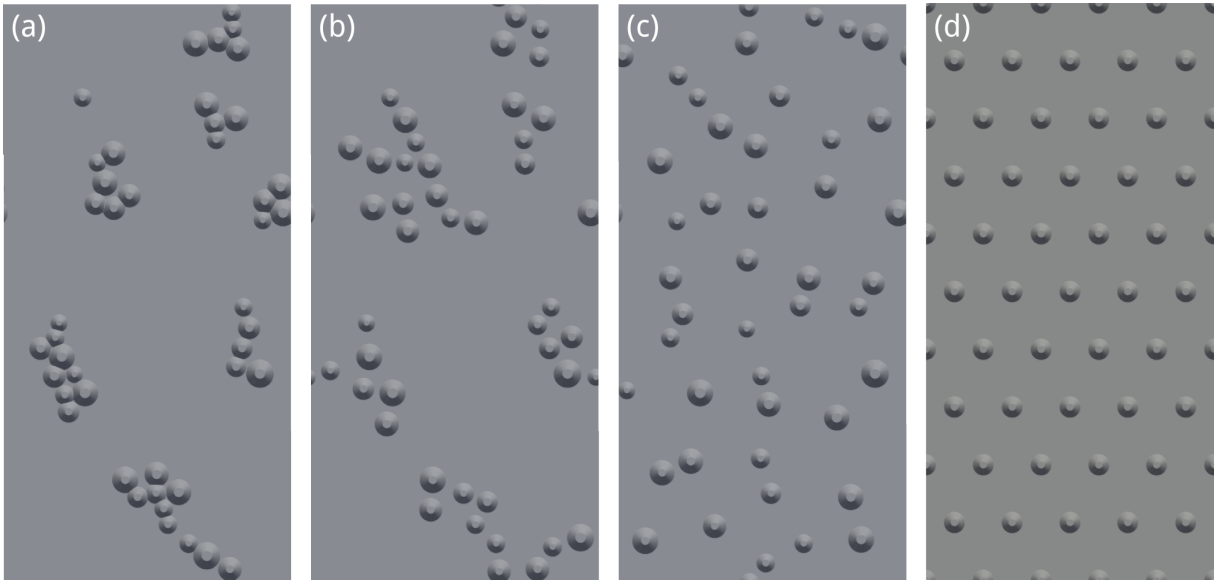
Figure 1. The four different barnacle-type rough surfaces: (a) case 1 - high degree of clustering; (b) case 2 - medium degree of clustering; (c) case 3 - low degree of clustering; (d) staggered regular arrangement.
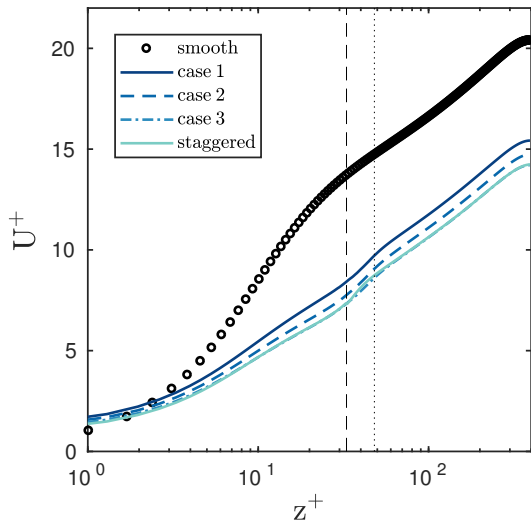

Figure 2. Mean streamwise velocity profiles. The vertical dashed line indicates the location of the average height of the barnacles h_{ave}^b and the vertical dotted line the maximum barnacle height h_{max}^b.

is attained just above the height of the highest barnacle. The profiles for case 3 and the regular staggered case are almost identical, indicating that a regular staggered arrangement is a good proxy for a homogeneous random arrangement of roughness elements when considering mean flow statistics. The velocity defect profiles, shown in figure 3 (a), collapse in all rough cases onto the smooth wall profile in the outer layer indicating that outer similarity is recovered.

The fluctuations of the velocity field have been separated into the turbulent fluctuations around the local mean (Reynolds stresses) and the spatial variations of the time-averaged velocity field that give rise to the dispersive stresses. Like the velocity defect profile, the streamwise normal Reynolds stress $\langle u'u' \rangle$ shows a good collapse on the smooth wall case in the outer layer (see figure 3 (b)). In the near-wall region $\langle u'u' \rangle$ is reduced compared to the smooth wall-case with case 1 maintaining the highest level of streamwise velocity fluctuations. This is consistent with the observation that this surface yields the lowest roughness function. The profile for case 1 shows two peaks in the near-wall region. The inner of these peaks occurs approximately at the location of the smooth-wall peak and is not found for case 2 and case 3 or the staggered case. This can be attributed to the larger connected smooth-wall areas for case 1, which appear to enable the recovery of a smooth-wall viscous sub-layer over parts of the surface. For all other cases, only a single peak can be observed, which is located between the average and the maximum barnacle height, i.e. close to the top of the barnacles. In the lower part of the roughness layer, the lowest levels of the streamwise Reynolds shear stress are observed for case 3 and the staggered surface.

The streamwise dispersive stress, shown in figure 3 (c), peaks for all three surfaces within the roughness layer at approximately half of the maximum barnacle height. The peak values observed exceed the peak streamwise Reynolds stresses in all cases. Case 1 gives rise to the highest streamwise dispersive stresses. This may be caused by the higher average streamwise velocity attained in the roughness layer for this case combined with the larger connected wake areas (and thus high local velocity deficits) formed behind the clusters of barnacles that characterise this surface (see also figure 6). Above the highest barnacle, the streamwise dispersive stresses quickly drop to close to zero values. The staggered arrangement leads to the lowest values of $\langle \tilde{u}\tilde{u} \rangle$ above the surface, and case 1 shows the slowest drop in streamwise dispersive stress. Compared to homogeneous random arrangement of roughness elements a regular arrangement will slightly underpredict the level of streamwise dispersive stress above the roughness layer.

The effect of the roughness on the spanwise and wall-normal Reynolds stresses is far weaker than on the streamwise Reynolds stress (see figure 4 (a) and (b)). A higher peak value of the spanwise Reynolds stresses can be ob-
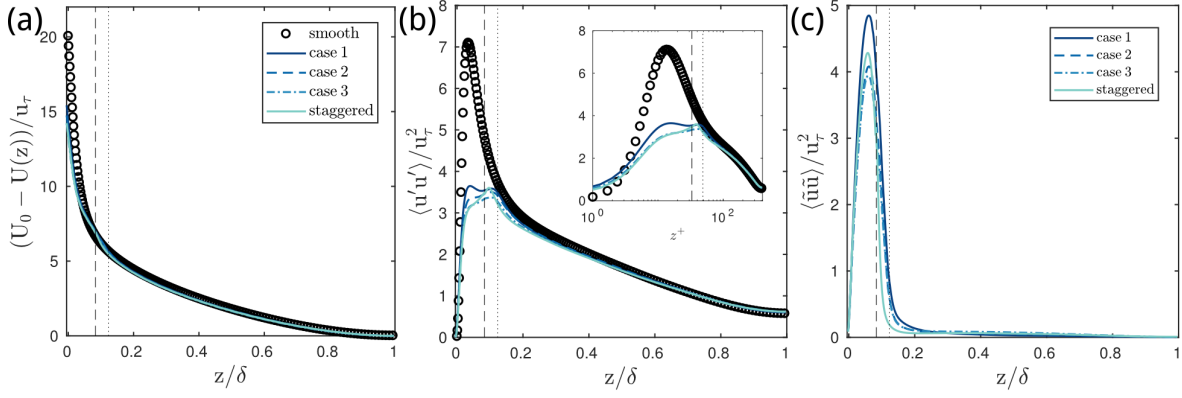
3

Figure 3. (a) Velocity defect profile; (b) streamwise normal Reynolds stress - legend see part (a) of figure; (c) streamwise dispersive stress. The vertical dashed line indicates the location of the average height of the barnacles h_{ave}^b and the vertical dotted line the maximum barnacle height h_{max}^b.
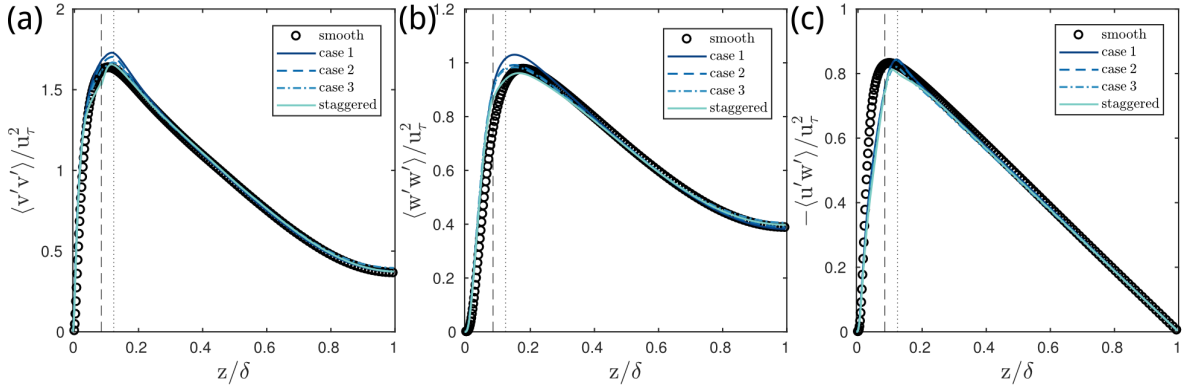

Figure 4. (a) Spanwise normal Reynolds stress; (b) wall-normal Reynolds stress; (c) Reynolds shear stress. The vertical dashed line indicates the location of the average height of the barnacles h_{ave}^b and the vertical dotted line the maximum barnacle height h_{max}^b.

served for the cases with significant clustering. Similarly, strong clustering also appears to promote wall-normal velocity fluctuations, whereas a regular staggered arrangement leads to a reduction of the peak value compared to the smooth wall case. The peak of the Reynolds shear stress $-\langle u'w' \rangle$ is shifted to approximately the height of the highest barnacle h_{max}^b and a reduction of the Reynolds shear stress can be observed in the near-wall layer (see figure 4 (c)).

The spanwise dispersive stresses, shown in figure 5, are significantly weaker than their Reynolds stress counterparts. The homogeneous random distribution of barnacles (case 3), gives rise to the highest spanwise dispersive stresses within the roughness layer. The peak occurs close to the base of the barnacle roughness elements, indicating that the mean flow is inclined to circumnavigate distributed barnacles rather than to be diverted over a barnacle roughness element. As for the streamwise dispersive stresses, the most clustered arrangement (case 1) sustains the highest spanwise dispersive stresses above the roughness sub-layer and the staggered arrangement leads to the weakest level of disturbance in the time-averaged spanwise velocity for $z > \max(h(x,y))$.

The wall-normal dispersive stresses show the lowest levels of the dispersive normal stresses, reaching less than

20% of the peak value of the wall-normal Reynolds stresses (see figure 5(c)). The staggered arrangement shows a sharp peak around the height of the barnacle elements for this surface with a steep drop-off above the roughness elements. The peak values for the three random arrangements are of similar magnitude and lower than for the staggered arrangement. Above the roughness, the slowest drop in dispersive stress is observed for case 1. This indicates that coherent clusters of barnacles may excite some weak larger-scale structures in the flow, that thus reach further into the outer layer of the mean flow.

The dispersive shear stress $-\langle \tilde{u}\tilde{w} \rangle$, shown in figure 5 (c), attains its highest values in the lower part of the roughness layer below h_{min}^b. This peak increases with increasing ΔU^+ for the random cases, a trend that is consistent with observations made for pit-peak decomposed irregular rough surfaces (Jelly & Busse, 2018). The near-wall peak for the staggered arrangement exceeds the level of all other cases. In the upper part of the roughness layer the profiles of the dispersive stresses then undergo a reversal to a minimum around the height of the highest barnacle before decaying to zero in the outer layer.

To gain further insight into the effect of clustering on the mean flow, the time-averaged mean streamwise veloc-
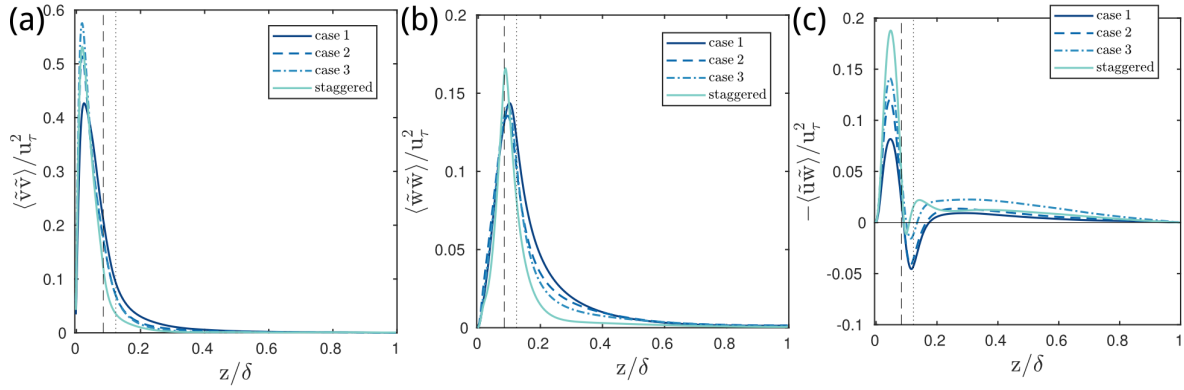
Figure 5. (a) Spanwise dispersive stress; (b) wall-normal dispersive stress; (c) dispersive shear stress. The vertical dashed line indicates the location of the average height of the barnacles h_{ave}^b and the vertical dotted line the maximum barnacle height h_{max}^b.
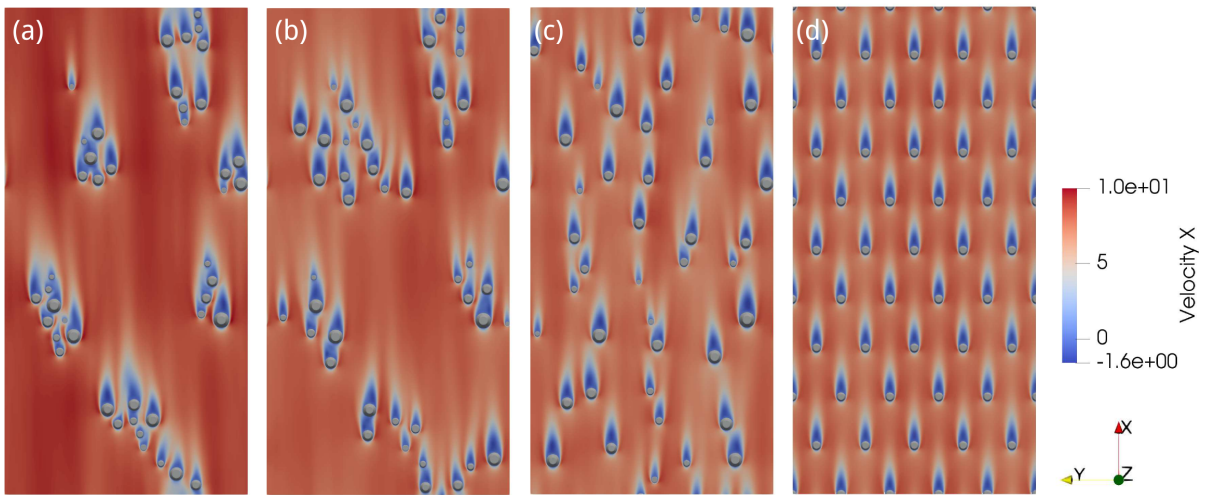

Figure 6. Time-averaged streamwise velocity scaled with u_τ on a horizontal plane located at $z \approx h_{min}^b$. (a) case 1, (b) case 2, (c) case 3, and (d) staggered.

ity field within the roughness layer has been visualised in figure 6. For the cases with significant clustering (case 1 and 2) significant shielding effects can be observed. Barnacles within a cluster that have upstream neighbours are therefore exposed on average to lower mean streamwise velocity. This also means that larger connected areas of very low mean streamwise velocity can form within the rough surface. In contrast, for case 3 almost all barnacles have their own distinct wake patterns, with a small area of low streamwise velocity on their downstream side. This is similar to the pattern that develops over the regular staggered rough surface.

Similar observations can be made when considering vertical cuts through the time-averaged streamwise velocity field (see figure 7). The wake patterns formed behind barnacles in case 3 and the staggered cases are very similar and only minimal impingement of the wake on downstream barnacles can be seen. In contrast, for case 2 and more so for case 1 the merging of wakes within a cluster can be observed. Thus for strongly clustered cases the individual barnacle acts as part of a larger obstacle to the flow and loses its individual aerodynamical identity. This causes inhomogeneities in the mean flow over larger (horizontal) length scales, and thus may also induce a higher level of

dispersive stresses above the roughness sub-layer compared to the homogeneous random and the regular staggered arrangements.

CONCLUSIONS

Some surface roughness generation processes, such as the colonisation of a surface by barnacles, lead to clustering, i.e. non-uniform distribution of the roughness features. By comparing the mean flow and turbulence statistics for three surfaces with different degrees of clustering but identical planform and frontal solidities, we found that the clustering of roughness elements has measurable impact on the fluid dynamic roughness effect of a surface with the case with the strongest clustering giving the lowest ΔU^+. Uniform regular staggered arrangements, as have been used in many previous studies, give a surprisingly good prediction for the effect of a homogeneous random arrangement of roughness elements, with an almost exact match of the mean streamwise velocity profile. Differences induced by strong versus weak degree of clustering can also be observed in the Reynolds and dispersive stress statistics. The most distinct effects of clustering are here the elevated peak levels of the spanwise and wall-normal Reynolds stresses and the higher
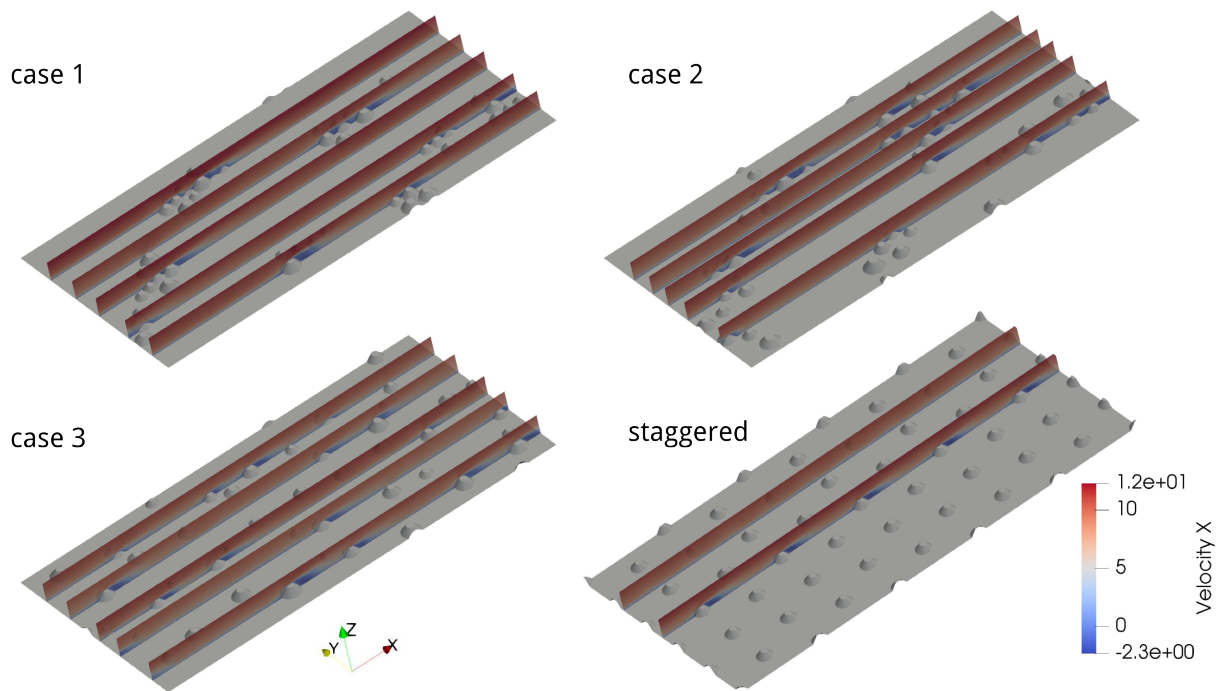
Figure 7.   Mean streamwise velocity contours (scaled with u_τ) on x-z planes at various spanwise locations.

levels of the dispersive normal stresses above the roughness.

For the given cases the difference between the mean flow and turbulence statistics of the cases with high compared to the cases with weak clustering are clearly discernible but overall not very high. We expect that the degree of clustering would have a much stronger influence for very sparse surfaces, i.e. for very low planform solidities $\lambda_p \ll 0.1$. In future, it would therefore be of interest to extend the current investigation on the influence of clustering of roughness elements to the limit of very low planform solidities.

REFERENCES

Barros, J. M., Murphy, E. A. & Schultz, M. P. 2016 Particle image velocimetry measurements of the flow over barnacles in a turbulent boundary layer. In *18th International Symposium on the Application of Laser and Imaging Techniques to Fluid Mechanics*.

Busse, A., Lützner, M. & Sandham, N. D. 2015 Direct numerical simulations of turbulent flow over rough surface based on a surface scan. *Computers & Fluids* **116**, 129–147.

Jelly, T. O. & Busse, A. 2018 Reynolds and dispersive shear stress statistics above highly skewed roughness. *Journal of Fluid Mechanics* **852**, 710–724.

Knight-Jones, E.W. & Crisp, D.J. 1953 Gregariousness in barnacles in relation to the fouling of ships and to antifouling research. *Nature* **171** (4364), 1109–1110.

Sadique, J., Yang, X. I., Meneveau, Ch. & Mittal, R. 2015 Simulation of boundary layer flows over biofouled surfaces. In *22nd AIAA Computational Fluid Dynamics Conference*.

Sarakinos, S. & Busse, A. 2019 An algorithm for the generation of biofouled surfaces for applications in marine hydrodynamics. In *Progress in CFD for Wind and Tidal Offshore Turbines (in preparation)* (ed. A. de Montlaur & E. Ferrer). Springer.

Schlichting, H. 1936 Experimentelle Untersuchungen zum Rauhigkeitsproblem. *Ingenieur-Archiv* **7**, 1–34.

Schultz, M. P. 2004 Frictional resistance of antifouling coating systems. *Journal of Fluids Engineering* **126** (6), 1039–1047.

Schultz, M. P., Bendick, J. A., Holm, H. R. & Hertel, W. M. 2011 Economic impact of barnacle fouling on a naval surface ship. *Biofouling* **27** (1), 87–89.